Palladium−Arene Interactions in Catalytic Intermediates: An Experimental and Theoretical Investigation of the Soft Rearrangement between η^1 and η^2 Coordination Modes

Marta Catellani,*,† Carlo Mealli,*,‡ Elena Motti,† Paola Paoli,§
Enrique Perez-Carreño,‖ and Paul S. Pregosin⊥

*Contribution from the Dipartimento di Chimica Organica e Industriale dell'Università,
Università di Parma, Viale delle Scienze, I-43100 Parma, Istituto per lo Studio della
Stereochimica ed Energetica dei Composti di Coordinazione, CNR, Via J. Nardi 39,
50132 Firenze, Italy, Dipartimento di Energetica Sergio Stecco, Università di Firenze,
Via di S. Marta 3, 50139, Firenze, Italy, Departamento de Química Física y Analítica,
Universidad de Oviedo, Spain, and Inorganic Chemistry ETH Zürich, Universitätstrasse 6,
CH-8092 Zürich, Switzerland*

Received July 11, 2001

Abstract: A series of dichloro-bridged arylbicycloheptylpalladium complexes have been synthesized and characterized by means of NMR spectroscopy. The compound $[(C_{16}H_{19})PdCl]_2 \cdot CH_2Cl_2$ with ortho and para methyl substituents at the arene has been characterized by means of X-ray diffraction techniques. The C_{ipso} atom of the arene lies almost at the fourth planar coordination site of the metal [$Pd-C_{ipso}$ = 2.22(1) Å (average)], and due to the arene's tilting, the substituted C_{ortho} atom is relatively close to the metal atom [2.54(1) Å (average)]. The coordinated $C_{ipso}-C_{ortho}$ linkage, in a seemingly dihapto coordination, is anti with respect to the CH_2 bridge of the bicycloheptyl unit. Variable-temperature NMR experiments for the para-substituted dimer **9** reveal restricted rotation of the two aryl groups about the corresponding $C-C_{ipso}$ bonds ($\Delta E \leq 17$ kcal mol^{-1}). DFT-B3LYP calculations have been carried out on the known and similar monomer (phenylbicycloheptenyl)Pd(PPh$_3$)I (**4**) and its related substituted derivatives. The essential results are as follows: (i) The potential energy surface for twisting the phenyl ring away from the symmetric η^1 coordination in **4** is very flat ($\Delta E \leq 1$ kcal mol^{-1}) whereas an *Atoms in Molecules* analysis excludes the existence of an actual $Pd-C_{ortho}$ bond in the seemingly η^2-type conformer. (ii) Complete rotation of the unsubstituted phenyl ring is not facile but feasible. A significant strain affects the transition-state structure featuring a $Pd-HC_{aryl}$ agostic-type bond. The calculated destabilization of 10.3 kcal mol^{-1}, with respect to the ground state, can be compared to the experimental barrier of the dimer **9**. (iii) Various methyl-substituted derivatives of **4** have been optimized, and their structural and energetic trends are discussed. An almost ideal η^1 coordination is shown by the anti conformer of the C_{ortho}-substituted complex due steric effects. For all of the other cases, a *slipped* η^2 coordination may be described. As a general conclusion, the unsaturated metal center receives π electron density of the arene mainly through its C_{ipso} atom. The effect may be slightly improved if the C_{ortho} atom also gets closer to the metal, but in no case, does the slipped η^2 coordination seem to be crucial for the stability of the system.

Introduction

Palladium σ-alkyl complexes resulting from insertion of bicycloheptene or bicycloheptadiene into Pd(II)−aryl bonds appear to be important intermediates in a variety of catalytic reactions involving C−H activation through palladacycles.[1] The equation in Chart 1, based on arylation chemistry, exemplifies the reaction sequence leading to *cis,exo*-arylalkylpalladacycles.

Compound **2** can give rise to several types of reactions such as ring formation with or without incorporation of other molecules.[2] In particular, **2** can undergo oxidative addition of

Chart 1
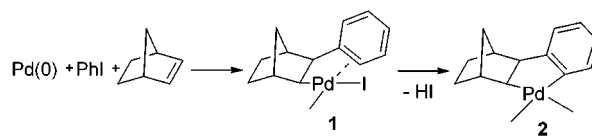
organic halides RX to form Pd(IV) complexes of type **3**, which have been isolated in the presence of appropriate ligands (Chart 2).[3]

Reductive elimination from complex **3** can readily occur through R migration to the aromatic ring when R is an alkyl group[4] but to the bicycloheptyl unit when R is an aryl group.[2] Interestingly, we have found that the migration of the latter can be directed selectively toward the aryl site of palladacycle **3** if the aromatic part of the latter carries a substituent at its ortho

† Università di Parma.
‡ ISSECC−CNR, Firenze.
§ Università di Firenze.
‖ Universidad de Oviedo.
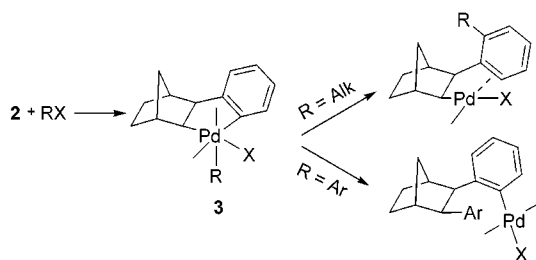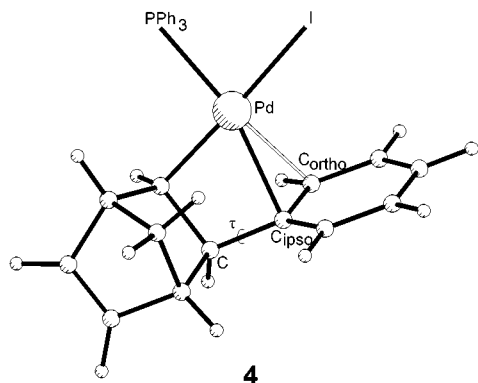⊥ ETH Zürich.

Chart 2

Chart 3

4

position.[5] New catalytic reactions have been derived from these observations.[6]

Study of the nature and reactivity of type **1** complexes, with substituents at the aromatic ring, appears of fundamental importance for mastering chemical syntheses involving their intermediacy. The extent of the partial interaction of the phenyl π system with the otherwise unsaturated Pd(II) ion remains poorly defined.

A significant contribution in this direction was provided by Cheng and co-workers, who reported the structure of the complex $(C_7H_8Ph)PdI(PPh_3)$ (**4**) schematized in Chart 3.[1a]

The geometry is such that the C_{ipso} atom of the phenyl ring occupies almost exactly the fourth planar coordination site of the metal. Tilting of the phenyl (τ rotation) permits one C_{ortho} atom to approach the metal. The resulting η^2 coordination of the corresponding $C_{ipso}-C_{ortho}$ linkage is asymmetric with the

Chart 4
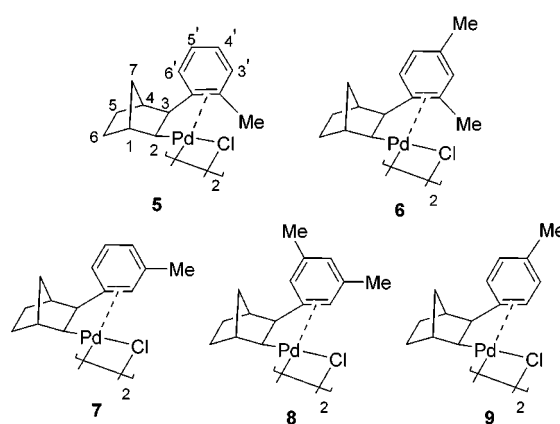
Pd−C_{ipso} and Pd−C_{ortho} distances being 2.43 and 2.59 Å, respectively. By contrast, in solution, rotation of the phenyl groups is observed by NMR. This is surprising as, when the phenyl ring lies in the coordination plane of palladium, the hydrogen atom bound to one C_{ortho} atom almost seems to collapse into the metal.

Consequently, there are a number of unresolved questions concerning the nature of the metal−phenyl bonding in **4** and other similar systems where the aryl coordination has been described as spanning the limits of the η^1/η^2 modes.[1a,7−11]

In the present paper, we present the syntheses and spectroscopy of new species that are related to **4**. In particular, the dimers **5−9**, which bear methyl groups at the various ortho, meta, and para aromatic positions, are described (Chart 4).

The structural analysis of *cis,exo*-3-(2′,4′-dimethylphenyl)-2-bicycloheptylpalladium chloride (**6**) is reported together with NMR data that suggest a somewhat different behavior between substituted and unsubstituted complexes. Further, DFT calculations (performed with package Gaussian98[12]) highlight the subtle (steric, electronic, or both) factors that control the η^1/η^2 dichotomy in this class of compounds.
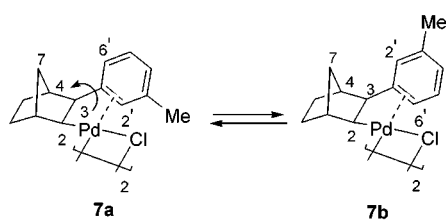
Results and Discussion

Synthesis and Characterization. Dimeric complexes **5−9** (Chart 4) containing one or two methyl groups in ortho, meta, and para positions were prepared by reaction of Li_2PdCl_4 with the corresponding arylmercuric chloride and bicycloheptene in acetonitrile at low temperature, according to a known proce-

(1) (a) Li, C.-S.; Cheng, C.-H.; Liao, F.-L.; Wang, S.-L. *J. Chem. Soc., Chem. Commun.* **1991**, 710. (b) Li, C.-S.; Jou, D.-C.; Cheng, C.-H. *Organometallics* **1993**, *12*, 3945. (c) Liu, C.-H.; Li, C.-S.; Cheng, C.-H. *Organometallics* **1994**, *13*, 18. (d) Catellani, M. In *Transition Metal Catalysed Reaction*; Davies, S. G., Murahashi, S.-I., Eds.; Blackwell Science: Oxford, 1999; p 169. (e) Catellani, M.; Chiusoli, G. P. *J. Organomet. Chem.* **1992**, *425*, 151. (f) Catellani, M.; Chiusoli, G. P. *J. Organomet. Chem.* **1992**, *437*, 369. (g) Markies, B. A.; Wijkens, P.; Kooijman, H.; Spek, A. L.; Boersma, J.; van Koten, G. *J. Chem. Soc., Chem. Commun.* **1992**, 1420. (h) Portnoy, M.; Ben-David, Y.; Rousso, I.; Milstein, D. *Organometallics* **1994**, *13*, 3465.
(2) (a) Catellani, M.; Chiusoli, G. P. *J. Organomet. Chem.* **1985**, *286*, C13. (b) Catellani, M.; Chiusoli, G. P.; Castagnoli, C. *J. Organomet. Chem.* **1991**, *407*, C30. (c) Catellani, M.; Marmiroli, B.; Fagnola, M. C.; Acquotti, D. *J. Organomet. Chem.* **1996**, *507*, 157. (d) Albrecht, K.; Reiser, O.; Weber, M.; Knieriem, B.; de Meijere, A. *Tetrahedron* **1994**, *50*, 383.
(3) (a) Catellani, M.; Chiusoli, G. P. *J. Organomet. Chem.* **1988**, *346*, C27. (b) Catellani, M.; Mann, B. E. *J. Organomet. Chem.* **1990**, *390*, 251. (c) Bocelli, G.; Catellani, M.; Ghelli, S. *J. Organomet. Chem.* **1993**, *458*, C12.
(4) Catellani, M.; Fagnola, M. C. *Angew. Chem., Int. Ed. Engl.* **1994**, *33*, 2422.
(5) (a) Catellani, M.; Motti, E. *New J. Chem.* **1998**, 759. (b) Catellani, M.; Motti, E.; Paterlini, L.; Bocelli, G.; Righi, L. *J. Organomet. Chem.* **1999**, *580*, 191. (c) Catellani, M.; Motti, E.; Paterlini, L. *J. Organomet. Chem.* **2000**, *593−594*, 240.
(6) (a) Catellani, M.; Frignani, F.; Rangoni, A. *Angew. Chem., Int. Ed. Engl.* **1997**, *36*, 119. (b) Catellani, M.; Cugini, F. *Tetrahedron* **1999**, *55*, 6595. (c) Catellani, M.; Motti, E.; Minari, M. *J. Chem. Soc., Chem. Commun.* **2000**, 157. (d) Lautens, M.; Piguel, S. *Angew. Chem., Int. Ed.* **2000**, *39*, 1045. (e) Catellani, M.; Motti, E.; Baratta, S. *Org. Lett.* **2001**, *3*, 3611.
(7) (a) Falvello, L. R.; Forniés, J.; Navarro, R.; Sicilia, V.; Tomás, M. *Angew. Chem., Int. Ed. Engl.* **1990**, *29*, 891. (b) Falvello, L. R.; Forniés, J.; Navarro, R.; Sicilia, V.; Tomás, M. *J. Chem. Soc., Dalton Trans.* **1994**, 3143.
(8) Cámpora, J.; López, J. A.; Palma, P.; Valerla, P.; Spillner, E.; Carmona, E. *Angew. Chem., Int. Ed.* **1999**, *38*, 147.
(9) Ossor, H.; Pfeffer, M.; Jastrzebski, T. B. H.; Stam, C. H. *Inorg. Chem.* **1987**, *26*, 1169.
(10) Forniés, J.; Menijón, B.; Gómez, N.; Tomás, M. *Organometallics* **1992**, *11*, 1187.
(11) Wehman, E.; van Koten, G.; Jastrzbeski, T. B. H.; Ossor, H.; Pfeffer, M. *J. Chem. Soc., Dalton Trans.* **1988**, 2975.
(12) Gaussian 98, Revision A.7: Frisch, M. J.; Trucks, G. W.; Schlegel, H. B.; Scuseria, G. E. M.; Robb, a.; Cheeseman, J. R.; Zakrzewski, V. G.; Montgomery, J. A.; Stratmann, R. E.; Burant, J. C.; Dapprich, s.; Millam, J. M.; Daniels, A. D.; Kudin, K. N.; Strain, M. C.; Farkas, O.; Tomasi, J.; Barone, V.; Cossi, M.; Cammi, R.; Mennucci, B.; Pomelli, C.; Adamo, C.; Clifford, S.; Ochterski, J.; Petersson, G. A.; Ayala, P. Y.; Cui, Q.; Morokuma, K.; Malick, D. K.; Rabuck, A. D.; Raghavachari, K.; Foresman, J. B.; Cioslowski, J.; Ortiz, J. V.; Stefanov, B. B.; Liu, G.; Liashenko, A.; Piskorz, P.; Komaromi, I.; Gomperts, R.; Martin, R. L.; Fox, D. J.; Keith, T.; Al-Laham, M. A.; Peng, C. Y.; Nanayakkara, A.; Gonzalez, C.; Challacombe, M.; Gill, P. M. W.; Johnson, B. G.; Chen, W.; Wong, M. W.; Andres, J. L.; Head-Gordon, M.; Replogle, E. S.; Pople, J. A. Gaussian, Inc., Pittsburgh, PA, 1998.

Chart 5

7a ⇌ **7b**

complex	C$_{ipso}$	C2′	C3′	C4′	C5′	C6′
5	81.7	135.8	126.4	130.9	130.9	127.8
6	78.8	136.5	132.1	142.6	128.0	129.4
7a	86.5	108.8	142.2	130.8	131.7	127.4
7b	86.5	129.7^b	141.8	132.6	131.7	106.2^b
8	87.7	104.7	142.4	137.5	142.7	126.3
9	82.0	110.8	130.7	142.1	132.7	131.0

^{a} Spectra were recorded in CDCl$_3$ at 298 K and are reported in ppm using the solvent signal ($\delta = 77$) as reference. ^{b} Owing to rotation (Chart 5), C6′ becomes the coordinated ortho carbon.

Chart 6

6′   **7′**

dure.[13] The resulting yellow compounds were characterized by NMR and mass spectra; the solid-state structure of **6** was determined by X-ray crystallography.

As previously reported by Cheng and co-workers,[1a−c] complexes of this type show dynamic behavior due to the possible rotation around the aromatic to aliphatic C−C bond, and usually their NMR spectra are temperature dependent. The presence of alkyl substituents, however, can introduce some rigidity. In particular, when a methyl group is present in the ortho position of the aromatic ring as in complexes **5** and **6**, rotation is hindered at room temperature and only the conformation with the methyl group pseudoanti to the bridge carbon atom (C7[14]) is observed. This is clearly indicated by NOESY spectra, which show cross-peaks corresponding to *o*-CH$_3$/H2, *o*-CH$_3$/H3, H6′/H4, and H6′/H7 syn contacts. Interestingly, the ^{1}H spectra of complexes **8** and **9** show two broad signals for the ortho protons H2′ and H6′, suggesting relatively slow rotation around the C−C bond at room temperature. In particular, the two ortho protons (H2′, H6′) of *p*-methyl-substituted complex **9** reveal a coalescence temperature of 313 K from which an energy barrier of ∼17 kcal mol^{-1} can be calculated.

The NMR spectra of meta-substituted complex **7** at room temperature show two rotationally non-equivalent conformers, **a** and **b**, in ∼2:1 ratio which remains unchanged up to 40 °C (Chart 5).

Lowering the temperature to −60 °C allows conformers **a** and **b** to be identified via the cross-peaks between H2′/H3, H2′/H2, and H6′/H7 syn of conformer **a** and those between H6′/H3 and H2′/H7 syn of conformer **b**. In the NOESY spectra recorded at room temperature, both aromatic protons H2′ and H6′ of conformers **a** and **b** show cross-peaks with the aliphatic protons H3, H4, and H7 syn, thus supporting the rotation indicated in the chart. Further evidence comes from exchange spectroscopy (EXSY). Cross-peaks in phase with those of the diagonal are observed in the NOESY spectra of complexes **7**, **8**, and **9** at room temperature, thus indicating chemical exchange. Particularly significant are the exchange peaks between H2′ and H6′ of complex **8** and those between H6′A/H6′B, H2′A/H2′B, and CH$_3$(A)/CH$_3$(B) of complex **7**. The intensity of the exchange cross-peaks varies, as expected, with temperature and is observed to be stronger at higher temperature and weaker at lower temperature.

^{13}C{^{1}H} NMR spectra of **5**−**9** were recorded in CDCl$_3$ at 298 K, and chemical shifts of the aromatic carbons are reported in Table 1.
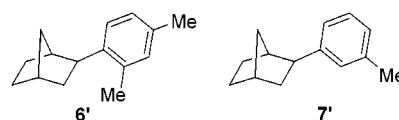
For **7**−**9**, the two palladium coordinated carbons (C$_{ipso}$ and C2′) appear at relatively low frequency in the region of 82.0−87.7 and 104.7−110.8 ppm, respectively. However, the spectra

of the *o*-methyl complexes **5** and **6** show only a single resonance at low-frequency assigned to the C$_{ipso}$ atom (81.7 and 78.8 ppm, respectively), while their ortho carbons (C2′) resonate at 135.8 and 136.5 ppm.

Further information comes from the comparison between the aromatic carbon chemical shifts of complexes **6** and **7** and the corresponding 2-arylbicycloheptane derivatives **6′** and **7′** (Chart 6).

A shift to low frequency of ∼60 ppm for the ipso carbon and one of ∼19 ppm for the ortho carbon C2′ is found by comparison of the signals of complex **7** with those of the corresponding organic compound, *exo*-2-(3′-methylphenyl)-bicycloheptane (**7′**). These data suggest an unsymmetrical η^2 coordination as reported by Cheng and co-workers.[1a] A comparison of **6** and the corresponding *exo*-2-(2′,4′-dimethylphenyl)-bicycloheptane (**6′**) reveals a low-frequency shift of ∼64 ppm for the ipso carbon, while the ortho carbon C2′ of both compounds (**6**, **6′**) resonates practically at the same frequency (δ 136.5 and 136.0 ppm, respectively). Similar conclusions can be drawn from the comparison of the remaining complexes (**5**, **8**, **9**) with the corresponding 2-arylbicycloheptane derivatives. These results suggest that, in solution, the coordination modes for ortho-substituted and ortho-unsubstituted complexes are somewhat different. In **7**−**9**, the metal affects both the ipso and ortho carbons, whereas in complexes **5** and **6**, with an ortho substituent, only the ipso carbon atom seems to be affected, suggesting η^1 to be a better description.

Structure of [(C$_{15}$H$_{19}$)PdCl]$_2$·CH$_2$Cl$_2$ (6). An ORTEP view of the complex dimer **6** is depicted in Figure 1. Crystal data are summarized in Table 2, and a selection of bond distances and angles is presented in Table 3.

The crystal structure consists of dimeric units where two Pd-(II) ions are held together by two chloride bridges. Moreover, there is a disordered dichloromethane solvent molecule that is joined to its centrosymmetric equivalent by a C−H⋯Cl hydrogen-bonding network. The metal dimer has non-crystallographic C_2 symmetry with the 2-fold axis perpendicular to the Pd$_2$Cl$_2$ plane. The chloride bridges are significantly asymmetric with the average Pd−Cl distances being 2.346(3) and 2.532(3) Å, respectively. The differences reflect the relative influence of the ligands in trans positions, namely, the alkyl carbon atom and the weakly bound arene. The local metal

(13) Horino, H.; Arai, M.; Inoue, M. *Tetrahedron Lett*. **1974**, 647.
(14) The atomic numbering of complex **5** shown in Chart 4 is used for the assignment of the NMR peaks and in the discussion.
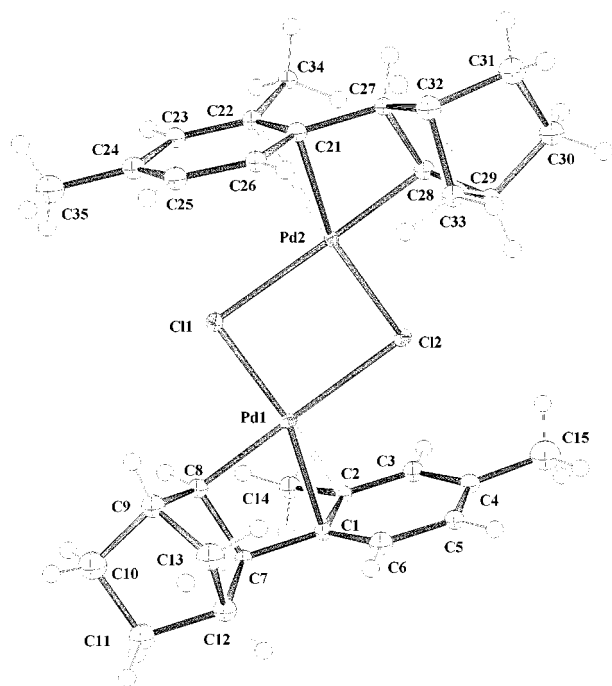
Figure 1. Molecular structure of [(C$_{15}$H$_{19}$)PdCl]$_2$.CH$_2$Cl$_2$ (**6**) showing the crystallographic labeling scheme.

Table 2. Crystal Data and Structure Refinement for [(C$_{15}$H$_{19}$)PdCl]$_2$.CH$_2$Cl$_2$ (**6**)

empirical formula	C$_{31}$ H$_{40}$ Cl$_4$ Pd$_2$
formula weight	767.23
temperature	100 K
wavelength	1.54180 Å
crystal system, space group	monoclinic, $P2_1/n$
unit cell dimensions	a = 11.785(5) Å, α = 90.0 deg.
	b = 21.824(5) Å, β = 115.962(5) deg.
	c = 12.937(5) Å, γ = 90.0 deg.
volume	2992(18) Å^3
Z	4
calculated density	1.703 mg/cm^3
absorption coefficient	13.127 mm^{-1}
$F(000)$	1544
crystal size	0.12 × 0.10 × 0.08 mm
ϑ range for data collection	4.05°−58.82°
limiting indices	−12<=h<=11, 0<=k<=23, 0<=l<=13
reflections collected/unique	11343/4000
completeness to θ = 58.82	93.3%
max and min transmission	0.4198 and 0.3018
refinement method	Full-matrix least-squares on F^2
data/restraints/parameters	3221/14/183
goodness of fit on F^2	1.135
final R indices [$I > 2\sigma(I)$]	R1 = 0.0746, wR2 = 0.1589
R indices (all data)	R1 = 0.0984, wR2 = 0.1701
extinction coefficient	0.00018(5)

coordination can be described by considering the T-shaped fragment formed by the two chloride bridges and by the carbanionic atom of the bicycloheptyl ligand. Thus, the unsaturated d^8 metal directs its σ hybrid to the C$_{ipso}$ atom of the phenyl substituent of the latter ligand. Remarkably, the torsion at the C$_7$−C$_8$ linkage, which controls the shift of the C$_{ipso}$ atom out of the metal coordination plane, is only 7°. The latter τ_1 value is the smallest among the few structures of this type present in the Cambridge Structural Database[15] and conveniently summarized in Table 4.

(15) Cambridge Structural Database System, version 5.20, Cambridge Crystallographic Data Centre, 12 Union Rd., Cambridge, CB2 1EZ, U.K.

Table 3. Selected Bond Lengths (Å) and Angles (deg) for the Complex [(C$_{15}$H$_{19}$)PdCl]$_2$.CH$_2$Cl$_2$ (**6**)^a

Pd(1)−Cl(1)	2.344(3)	C(8)−Pd(1)−C(1)	69.0(5)
Pd(1)−Cl(2)	2.533(3)	C(8)−Pd(1)−Cl(1)	93.4(4)
Pd(2)−Cl(1)	2.532(3)	C(1)−Pd(1)−Cl(1)	162.2(3)
Pd(2)−Cl(2)	2.348(3)	C(8)−Pd(1)−Cl(2)	177.9(4)
Pd(1)−C(8)	2.02(1)	C(1)−Pd(1)−Cl(2)	111.0(3)
Pd(1)−C(1)	2.24(1)	Cl(1)−Pd(1)−Cl(2)	86.5(10)
Pd(1)−C(2)	2.57(1)	C(8)−Pd(1)−C(2)	85.5(4)
Pd(2)−C(28)	2.03(1)	C(1)−Pd(1)−C(2)	34.1(4)
Pd(2)−C(21)	2.21(1)	Cl(1)−Pd(1)−C(2)	152.2(3)
Pd(2)−C(22)	2.52(1)	Cl(2)−Pd(1)−C(2)	95.5(3)
C(1)−C(7)	1.58(2)*	C(28)−Pd(2)−C(21)	69.0(5)
C(1)−C(6)	1.40(2)*	C(28)−Pd(2)−Cl(2)	94.6(4)
C(1)−C(2)	1.44(2)*	C(21)−Pd(2)−Cl(2)	162.2(3)
C(2)−C(3)	1.37(2)*	C(28)−Pd(2)−C(22)	85.9(4)
C(3)−C(4)	1.38(2)*	C(21)−Pd(2)−C(22)	34.5(4)
C(4)−C(5)	1.40(2)*	Cl(2)−Pd(2)−C(22)	156.1(3)
C(5)−C(6)	1.37(2)*	C(28)−Pd(2)−Cl(1)	178.9(3)
C(2)−C(14)	1.52(2)*	C(21)−Pd(2)−Cl(1)	110.0(3)
C(4)−C(15)	1.48(2)*	Cl(2)−Pd(2)−Cl(1)	86.4(1)
		Pd(1)−Cl(1)−Pd(2)	93.5(1)
		Pd(2)−Cl(2)−Pd(1)	93.4(1)
		C(7)−C(1)−C(2)	120.2(9)*
		C(7)−C(1)−C(6)	123.0(9)*
		C(2)−C(1)−C(6)	116.6(9)*

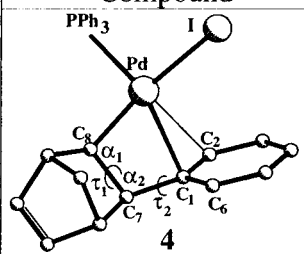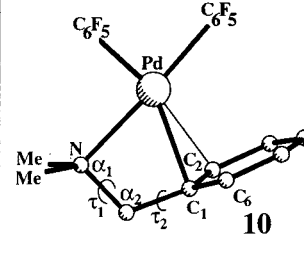^{a} The values with an asterisk are the average between the two equivalent units in the molecule.
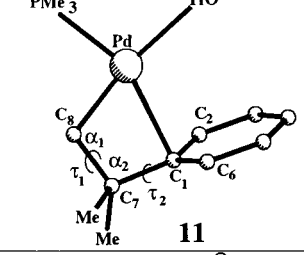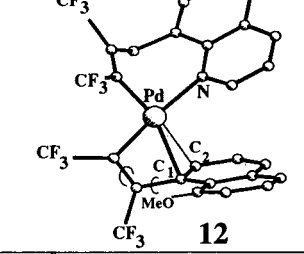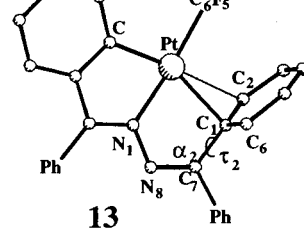
Moreover, the Pd−C$_{ipso}$ distance of 2.22(1) Å (average) is significantly shorter than in the analogous structures reported in Table 4 (observed range of 2.327−2.433 Å). It is also 0.11 Å shorter than in the Pd dimer, Pd$_2$(CH$_3$CN)$_2$(PPh$_3$)$_2$, where phosphine phenyl substituents use only their C$_{ipso}$ atoms to complete the local coordination of two joined Pd metals.[16] This suggests that, in our case, the η^1 coordination of the phenyl ring is most efficient although the weak trans influence exerted by chloride ligand must be taken into account. The methyl-substituted C$_{ortho}$ atom (C$_2$ or C$_{22}$) lies at relatively long distance from the metal [2.54(1) Å] although it is closer than the unsubstituted C$_{ortho}$ analogue (C$_6$ or C$_{26}$) [2.79(1) Å (ave)]. Such an asymmetric orientation of the arene can be parametrized by the torsion (τ_2) of the arene about the linkage, C$_7$−C$_1$ (or C$_{27}$−C$_{21}$).[17] While the ideal η^1 coordination corresponds to $\tau_2 = 90°$, the present value of 77(1)° is slightly smaller than the 82(1)° value found in the complex (PMe$_3$)(TfO)Pd(C$_6$H$_5$CMe$_2$CH$_2$) (**11**).[8] The latter, based on the similarity of Pd−C$_2$ and Pd−C$_6$ distances [2.66(1) and 2.71(1) Å, respectively], is the closest example to ideal η^1 coordination. Indeed, greater torsions toward η^2 are found for the other complexes listed in Table 4 with more asymmetric Pd−C$_2$ and Pd−C$_6$ distances. On the other hand, there are some indications of an effective slipping toward η^2 coordination in **6**. If, on one side, the large standard deviations make questionable the elongation of the vector C$_1$−C$_2$ (or C$_{21}$−C$_{22}$) with respect to the side of the arene's ring [1.44(2) vs 1.39(3) Å, averages], the pinning back of the methyl substituent at the C$_2$ (or C$_{22}$) atom is more significant. In fact, the corresponding tilt angle of 8.5(9)° is definitely larger than that of the other meta substituent [3.0(9)°].

A final remark concerns the orientation of the methyl group bound to the C$_{ortho}$ atom (C$_2$ or C$_{22}$). This may be of some

(16) Murahashi, T.; Otani, T.; Okuno, T.; Kurosawa, H. *Angew. Chem., Int. Ed.* **2000**, *39*, 537.
(17) Such a definition of the arene's twisting is undermined by the nonequivalence of the two angles C$_1$−C$_7$−C$_{ortho}$, which are somewhat greater (C$_{ortho}$ = C$_6$) or smaller (C$_{ortho}$ = C$_2$) than 120° (see Table 2).

Table 4. Selected Structural Features of Complexes Stabilized by Partial Interaction of the Arene's π System with an Unsaturated d^8 Ion (Pd or Pt) (Distances in Å and Angles in deg)

Compound	Geometry	
4	$Pd-C_1$	2.430(5)
	$Pd-C_2$	2.591(6)
	$Pd-C_6$	3.191(7)
	α_1	100(1)
	α_2	106(1)
	τ_1	8(1)
	τ_2	69(1)
	SOCRUX, 1a[a]	
Present dimer, **6**	$Pd-C_1$	2.22(1)
	$Pd-C_2$	2.54(1)
	$Pd-C_6$	2.79(1)
	α_1	96(1)
	α_2	103(1)
	τ_1	7(1)
	τ_2	77(1)
10	$Pd-C_1$	2.39(1)
	$Pd-C_2$	2.57(1)
	$Pd-C_6$	3.03(1)
	α_1	100(1)
	α_2	105(1)
	τ_1	17(1)
	τ_2	63(1)
	BIXFET, 7[a]	
11	$Pd-C_1$	2.34(1)
	$Pd-C_2$	2.66(1)
	$Pd-C_6$	2.71(1)
	α_1	91(1)
	α_2	114(1)
	τ_1	12(1)
	τ_2	82(1)
	VETZID, 8[a]	
12	$Pd-C_1$	2..433(3)
	$Pd-C_2$	2.571(5)
	$Pd-C_6$	3.210(5)
	α_1	104.3(3)
	α_1	112.0(4)
	τ_1	17(1)
	τ_2	69(1)
	FEXWEK, 9[a]	
13	$Pd-C_1$	2..327(6)
	$Pd-C_2$	2.611(6)
	$Pd-C_6$	2.910(7)
	α_2	124.5(7)
	τ_2	80(1)
	KOXSIZ, 10[a]	

[a]Refcode as given in the Cambridge Structural Database and original Reference. For **6** and **10**, the geometrical parameters are average between two equivalent units.

importance for the stability of the system (see the theoretical discussion below). As a matter of fact, the methyl's hydrogen

Chart 7

4a
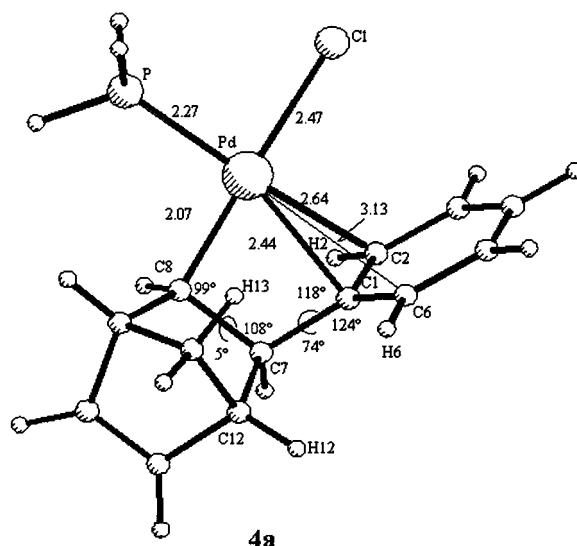
atoms did not show up from ΔF maps and were calculated. Remarkably, the arrangement shown in Figure 1, with one H atom constrained in the plane of the arene and pointing opposite to the bicycloheptenyl ligand, affords a slightly lower R factor (by ~0.1) as compared to the situation where the methyl group is rotated by 180°. Given the poor quality of the diffraction data, this result may appear insignificant but it acquires some meaning in view of the optimized computational model (vide infra).

Computational Analysis. For the sake of computational feasibility, our theoretical study of the $\eta^1-\eta^2$ dichotomy in palladium–arene complexes is based on the known monomer $(C_7H_8Ph)PdI(PPh_3)$ (**4**)[1a] rather than on the here-characterized dimers. Despite replacing PPh_3 and iodide with the PH_3 and chloride ligands, respectively, the optimized model **4a** (see Chart 7) is found to be in good agreement with the corresponding X-ray data.[1a]

For instance, the calculated $Pd-P$, $Pd-C_8$, $Pd-C_1$, and $Pd-C_2$ distances, reported in Chart 7, are comparable to those observed (2.25, 2.05, 2.43, and 2.59 Å, respectively).[1a] Moreover, the angles α_1, α_2, τ_1, and τ_2 (defined in Table 4) are in a relatively good agreement with those of the complex **4** (CSD[15] refcode: SOCRUX).

The calculated τ_1 torsion at the C_8-C_7 bond, which almost forces the C_{ipso} atom (C_1) to occupy the fourth square planar position of the metal, is even smaller than in the experiment[1a] (5° vs 8°). At the same time, the planes of the arene and the $PdC_8C_7C_1$ chelate deviate significantly from orthogonality and more so in the experimental structure (τ_2 being about 69° and 74° in **4** and **4a**, respectively). Such a twisting greatly differentiates the two $Pd-C_{ortho}$ separations (i.e., 2.64 vs 3.13 Å in **4a**) so that a bias toward the η^2 coordination must be considered. Even so, the latter is far from being achieved given the significant difference in the $Pd-C_{ortho}$ and $Pd-C_{ipso}$ separations. Also, the $C_{ipso}-C_{ortho}$ bond, which is potentially dihapto coordinated, is barely elongated with respect to its uncoordinated analogue (1.42 and 1.41 Å for C_1-C_2 and C_6-C_1, respectively). By contrast (as pointed out in the structural section), an idea of the degree of η^2 coordination may be gained from the amount
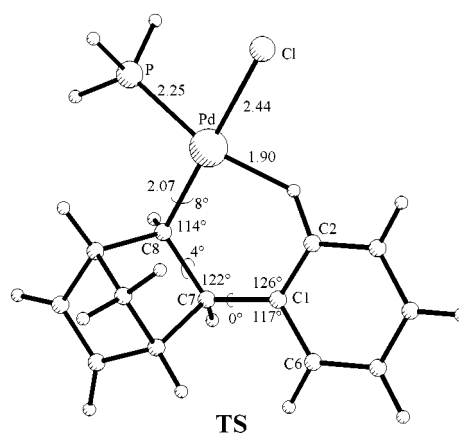
Chart 8

Chart 9

TS
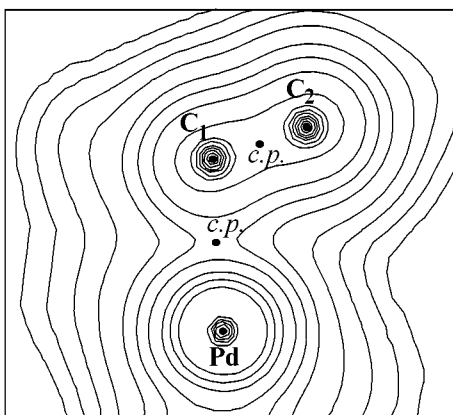
of pinning of the substituent at the C_{ortho} position. In this case, the H_2 atom appears uniquely bent away from the C_6 ring by ∼6°.

As an alternative conformation, the C_1-C_6 linkage could be biased toward dihapto coordination, the phenyl ring being tilted on the same side of the bicycloheptenyl bridge. However, based on the NMR analysis,[1b] the dichotomy between the syn and anti forms is not relevant. Indeed, a single-point calculation for the syn conformer (same geometry as **4a** with $\tau_2 = -80°$) indicated an energy destabilization of ∼30 kcal mol^{-1} with respect to the anti species. This is due to steric hindrance (e.g., a very short contact of 1.7 Å between H_6 atom and the H_{13} atom of the CH_2 bridge), which can be possibly relieved by adjusting other geometric parameters (vide infra). In any case, it is sufficient to reduce the twist of the ring by ∼5° (with the corresponding elongation of the $Pd-C_6$ distance from 2.6 to 2.8 Å) to reduce the energy gap to ≤3 kcal mol^{-1}. From this point, the energy profile proceeds smoothly downhill to the absolute minimum **4a** passing through the authentic η^1 structure. The latter, which has been fully optimized, after fixing τ_2 at 90°, is only 0.5 kcal mol^{-1} higher than **4a**. Its geometrical features are essentially identical to those of **4a** (Chart 7) with the obvious exception of the now equal $Pd-C_2$ and $Pd-C_6$ separations (2.93 Å).

In view of the flat potential energy surface (PES), oscillation of the unsubstituted phenyl ring between the η^2 and the η^1 arrangements can be an easy process in solution. The metal does not seem to receive significantly more electron density in the η^2 coordination mode. As shown from a comparison of the Mulliken analyses, the metal population increases at most by 0.014 electron. To better assess the nature of the $Pd-C_2$ bond, we carried out a topological analysis of the electron density for **4a** by using the theory of *Atoms in Molecules*[18] and the recently released AIM2000 program.[19] The electron density map in the plane of the triangle PdC_1C_2 is shown in Chart 8.

Bond critical points (of the type 3,−1) are observed between the atoms $Pd-C_1$ and C_1-C_2 but not along the path $Pd-C_2$. Nor is there any (3,+1) critical point within the PdC_1C_2 triangle. The electron density, which has the very low value of 0.05 e/Å^3 at the $Pd-C_1$ critical point, practically vanishes between the Pd and C_2 atoms. It may not be excluded that in the dimeric

(18) Bader, R. F. W. *Atoms in Molecules: A Quantum Theory*; Oxford University Press: New York, 1994.
(19) Biegler-König, F.; Schönbohm, J.; Bayles, D.; AIM2000: A Program to Analyze and Visualize Atoms in Molecules. *J. Comput. Chem.*, submitted.

species **6** where the equivalent $Pd-C_2$ separation is ∼0.1 Å shorter than in **4** or **4a**, a corresponding critical point may be detected. By contrast, it must be pointed out that in **6**, because of the methyl substituent at the C_{ortho} atom, the arene is less twisted about the exocyclic C_1-C_7 linkage (τ_2 being 77° and 69° in **6** and **4**, respectively). In conclusion, the AIM approach does not provide any significant evidence for the direct $Pd-C_2$ bond or for the delocalization of bonding over three atomic centers.

A steric problem in these molecules is evident even in the absence of methyl substituents at the phenyl group. This is highlighted by the fact that the bond angles at the C_{ipso} atom deviate significantly from the ideal sp^2 120°. In both **4** and **4a**, the angles $C_7-C_1-C_2$ and $C_7-C_1-C_6$ are about 118° and 124°, respectively. The latter distortion allows elongation to the reasonable values of 2.3−2.4 Å of the otherwise short contacts between the phenyl's H_6 atom and the H_{12} and the H_{13} atoms of the bicycloheptenyl group. Interestingly, cross-peaks between the same protons are always observed in the NOESY spectra of this type of compound.

Another intriguing steric problem concerns the complete rotation of the phenyl ring about the exocyclic C_7-C_1 linkage. This feature was first reported for **4** on the basis of NMR spectra at variable temperatures[1b] and is confirmed for **7−9**, which do not carry methyl substituents at their ortho positions.

Geometric modeling of the phenyl rotation process in **4a** was first made by allowing only τ_2 to vary between ±90° while fixing any the remaining geometric parameters. For $\tau_2 = 0°$ (i.e., when the Pd coordination plane and that of the phenyl ring coincide), the hydrogen bound to one C_{ortho} atom almost collapses into the metal (Pd−H ∼0.5 Å). Evidently, a significant structural rearrangement is needed to allow the phenyl to flip through the metal coordination plane. Full optimization of the transition state was performed (correctly characterized by a single imaginary frequency) and provided the structure depicted in Chart 9. This features a six-membered metallacycle where the inner angles at the sp^3 C_8 and C_7 atoms open up to 114° and 122°. The $C_7-C_1-C_2$ angle (<120° in the ground structure) now approaches 126°. In this manner, the Pd and H atoms avoid bumping into each other, and given their separation of 1.90 Å, direct bonding is not to be excluded.

Interestingly, the AIM analysis[18,19] of the TS structure reveals a critical point along the Pd−H vector, thus suggesting an unusual form of Pd−HC *agostic* interaction. The latter attraction should partially compensate the strain energy of the overall

Chart 10

4b

4c

Chart 11

4d

4e
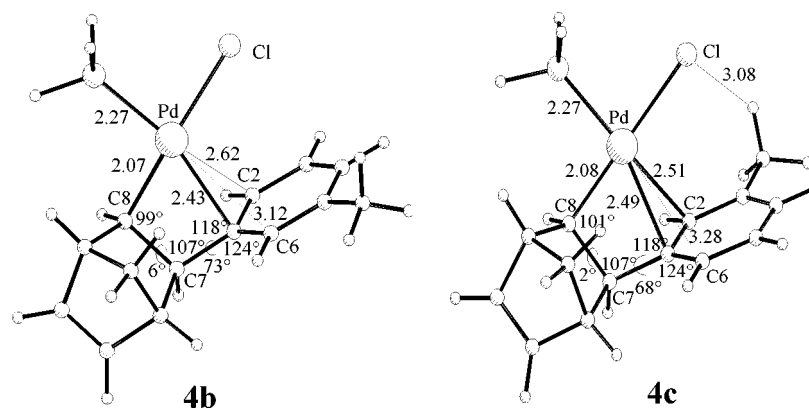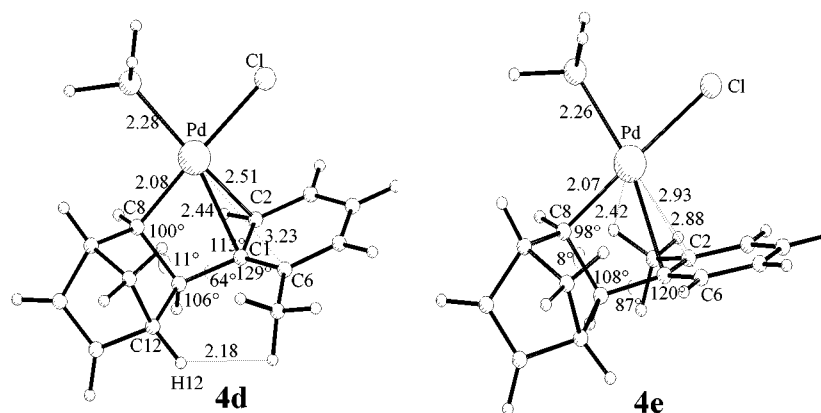
structure with a net energy balance of $+10.3$ kcal mol^{-1}. Such a significant barrier, calculated for the gaseous state, is anyway smaller than the 17 kcal mol^{-1} value experimentally determined for the dimer **9**. Clearly, the detection of the present TS structure may be a relevant key step for understanding the process that leads to the observed palladacycles.[2a]

To clarify the electronic or steric effects induced by the presence of one or two methyl substituents at the arene, we have optimized the structures of a few derivatives of the parent model **4a**. First, the pair of meta conformers **4b** and **4c** (see Chart 10) has been considered where the phenyl is substituted at either the syn or the anti position with respect to the bicycloheptenyl bridge. The anti species **4c** is only 0.8 kcal mol^{-1} more stable than its syn analogue **4b**. Even if this result is consistent with the 2:1 ratio indicated by NMR spectroscopy, the energy difference is insignificantly small for conformers **7a** and **7b**, respectively (Chart 5). Some geometric aspects are noteworthy. In **4c**, the Pd–C$_2$ distance is ∼0.11 Å shorter with a correspondingly different τ_2 torsion (68° vs 73°). This effect arises from the intramolecular Cl⋅⋅HC hydrogen bonding which is highlighted in the drawing **4c**.

Since the energetics of the hydrogen bond and that of the improved η^2 coordination are additive in this case, the insignificant gain with respect to the conformer **4b** is a further indication of the modest impact of the arene's dihapto versus monohapto bonding.

If a substituent at the meta position has no significant effect from the energetic point of view, the substitution at one of the ortho carbon atoms is clearly destabilizing. The syn and anti conformers **4d** and **4e**, shown in Chart 11, possess significantly

higher energy (7.7 and 3.4 kcal mol^{-1}, respectively) than the most stable meta derivative **4c**.

Steric strain in the syn species **4d** is indicated by the increased asymmetry of the sp^2 angles at the C$_{\text{ipso}}$ atom. In particular, C$_7$–C$_1$–C$_6$ opens up to 129° to minimize the repulsion between methyl and bicycloheptenyl H atoms (a still short H⋅⋅H contact of 2.18 Å is highlighted in the drawing). Thus, the most enhanced η^2 coordination ($\tau_2 = 64°$ and Pd–C$_2 = 2.51$ Å) is not sufficient to compensate the unfavorable strain.

The situation is significantly different in the anti isomer **4e** (Chart 11). The calculations show that the phenyl ring lies almost perpendicular to the Pd coordination plane ($\tau_2 = 87°$) and that the two separations Pd–C$_2$ and Pd–C$_6$ are equally long (2.90 Å average). Accordingly, the model suggests η^1 coordination mode to an even greater extent than in the experimental structure (PMe$_3$)TfOPd(CH$_2$CMe$_2$Ph) (**11**), where the phenyl ring is unsubstituted (see VETZID in Table 4). A more detailed observation of **4e** suggests that the twist toward η^1 relieves a short contact between the upper H atom of the methyl substituent and the Pd atom itself (indicated by the dotted line in Chart 11). Regardless of the latter observations, it would be wrong to conclude that an ortho methyl substituent in the anti position is a stabilizing factor for the coordination. Recall in fact that, under comparable circumstances, complex **6** features a τ_2 angle more twisted toward η^2 by ∼10°.

Finally, the optimized structure of the derivative with substituents at both the ortho positions (**4f** in Chart 12) shows again short H⋅⋅⋅H contacts between the bycycloheptenyl and the syn methyl group and the significant asymmetry of the sp^2 angles at C$_1$. As in **4d**, the effect could be that of shortening

Chart 12

4f
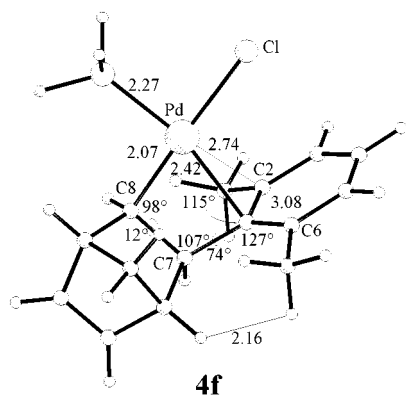
the Pd–C_2 distance and favoring the η^2 coordination mode of the C_1–C_2 linkage. By contrast, the anti methyl group pushes toward the η^1 coordination. Eventually, a compromise is reached at the τ_2 value of 74°, which is almost midway between those reported for **4d** and **4e**.

Another indication of the serious hindering problems that affect the structure **4f** are the large out-of-plane deviations of both the methyl groups (12° and 10° for those bound at the atoms C_2 and C_6, respectively). Under these circumstances, the pinning can hardly be an indicator of the C–C dihapto bonding itself.

Interestingly, the orientation of the anti methyl group described in **4e** and **4f** shows one H atom in the plane of the arene and opposite to the bicycloheptenyl ligand. If the methyl were 180° rotated, a very short contact would occur between the latter hydrogen and that bound to the atom C_8. According to this finding, also the questionable result obtained from the constrained least-squares refinement of **6** (see the structural section) carries more weight. Moreover, even the simplest Walsh diagrams, constructed with CACAO[20] and based on EHMO calculations,[21] show the existence of energy barriers of a few kilocalories per mole for the free rotation of the CH_3 group in the anti position. Not only at 180° but also at ±90°, the short contact of one of the methyl H atoms with a filled metal orbital is the cause of a four-electron repulsion.

It is clear that in the ground state of all of these molecules the electron saturation of the d^8 metal ion is achieved thanks to the π system of the arene, mainly through its C_{ipso} atom. Thus, a 90° rotation of the ring as in the TS structure (Chart 9) is attributable not only to the strained conformation of the ligand but also to the loss of the stabilizing π interaction. The "agostic-type" interaction, in the latter case, is no more than a meager compensation for the loss of Pd–C π-bonding. However, for a small range of τ_2 values (and possibly for the ideal η^1 conformation itself), it may not be excluded that some π electron density also flows toward the metal from the C_{ortho} atom. Qualitative MO arguments help to illustrate this point. By referring to the π system of C_6H_6, the degenerate set of filled π orbitals, shown in Chart 13, is the closest in energy (~2 eV) to the unique σ hybrid of the T-shaped Pd(II) fragment and it acts as the potential donor.

(20) (a) Mealli, C.; Proserpio, D. M. *J. Chem. Educ.* **1990**, *67*, 399. (b) Mealli, C.; Ienco, A.; Proserpio, D. M. *Book of Abstracts of the XXXIII ICCC*; Florence, 1998; P 510.
(21) (a) Hoffmann, R.; Lipscomb, W. N. *J. Chem. Phys.* **1962**, *36*, 2872. (b) Hoffmann, R.; Lipscomb, W. N. *J. Chem. Phys.* **1962**, *37*, 3489.

Chart 13

a   **b**

Chart 14

Chart 15

c   **d**
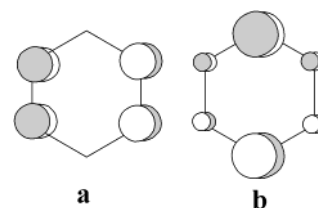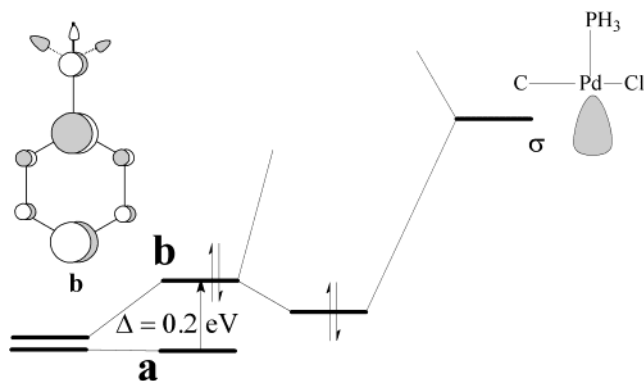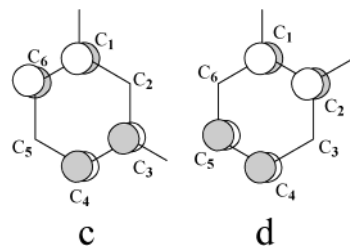
The two members **a** and **b** are equivalent for benzene but, in the presence of a single alkyl substituent (in our case, the bicycloheptenyl unit itself), **b** lies ~0.2 eV higher than **a** due to the orthogonal interaction of the π system with one of the alkyl σ-bonding combinations (see Chart 14). Thus, the interaction with **b** is favored by the reduced gap with respect to the metal σ hybrid.

Even if **b** is centered at the C_{ipso} atom, the metal receives a small contribution from the ortho carbon atoms and the effect is asymmetrically magnified upon the twisting of the ring and slippage toward η^2 coordination. Obviously, such a qualitative explanation of the orbital preferences, based on the symmetry distinction between **a** and **b**, is not rigorous as the twisting forces the mixing of the two components. Still, a reminiscence of the ideal situation remains which allows some interpretation of the effects of the substituents.

The presence of a second alkyl substituent, in either the meta or the ortho position, destabilizes preferentially the combination of type **a** as shown by the sketches in Chart 15.

A meta substituent at the atom C_3 (as in **4c**) should favor twisting toward the atom C_6, namely, toward the side of the bicycloheptenyl ligand. However, we have already pointed out that η^2 syn conformers have serious strain problems; moreover, H··Cl hydrogen bonding becomes operative as shown in **4c**. In conclusion, the electronic trend favoring the C_1–C_6 coordination may vanish in this case. On the contrary, if the meta substitution takes place at C_5 (imagine the mirror drawing with respect to **c** in Chart 15), η^2 coordination of C_2 is favored (see structure **4b**).
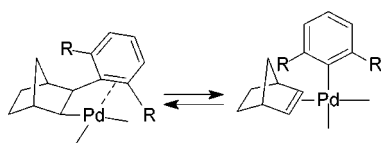
Chart 16

By considering next the two possible ortho substitutions, the drawing **d** in Chart 15 suggests that a substituted C_2 atom should favor the η^2 coordination of the C_1-C_2 linkage itself. This occurs in the experimental structure **6** (by overlooking the effect of the second substituent in para) although it is in contrast with the calculated η^1 structure **4e**. We have already pointed out for the latter that the short contact of a methyl H atom and the metal itself may disfavor the η^2 coordination in this case. Finally, the mirror image of **d** in Chart **15** suggests that substitution at atom C_6 should favor a syn η^2 conformer which is however sterically highly demanding even for the unsubstituted arene. In fact, the optimized species **4d** is by far the most destabilized of the series, confirming that both unfavorable electronic and steric effects sum up in this case.

Conclusions and Extensions

New dimeric species showing the forced interaction between a portion of an arene π system and an unsaturated Pd(II) metal have been investigated by means of NMR experiments and X-ray analysis for one of them (**6**). A rather flexible arrangement of the arene about the metal emerges. The C_{ipso} atom invariably occupies the fourth square planar coordination site of the metal, and it acts as the main donor of arene's π electron density. Twisting of the phenyl, which brings one C_{ortho} atom closer to metal, as well as other indicators of η^2 coordination (e.g., the pinning of the substituent at the C_{ortho} atom) have been highlighted for both the experimental and computed structures. Still, the dihapto coordination does not seem to be a driving force in these systems nor, from the computational viewpoint, could any Pd–C_{ortho} bonding interaction be detected by the *Atoms In Molecules*[18] method. The electronic energy, which may be gained at the *slipped* η^2 coordination, is small and is easily contrasted by steric hindrance involving the ortho arene's H atoms (or those of the methyl substituents), some bicycloheptenyl atoms, and possibly the metal itself.

The presence (or absence) of barriers to rotation has been monitored by NMR spectroscopy, and for one dimer, it has been measured to be $\sim$17 kcal mol^{-1}. On the other hand, the DFT calculations have permitted observation of the stereochemical and energetic features of the corresponding transition-state structure for a comparable monomeric model. This appears to be highly strained, although a compensating Pd–HC_{aryl} agostic-like interaction permits partial saturation of the metal and avoids larger destabilization. The characterization and the demonstrated energetic accessibility of the TS structure acquire a particular meaning with respect to the important reaction step connecting the present type of structures and palladacycles.[2a]

In this paper, we have not addressed the possibility for the *o*-R-disubstituted phenylbicycloheptylpalladium complexes to undergo bicycloheptene deinsertion, which leads to the η^2-bicycloheptene-σ-aryl species, schematically shown in Chart 16.[4,22] In the latter, saturation of the Pd(II) metal is achieved in

the most classic way via separated donations from both the π electrons of the *ene* and the σ *lone pair* of the phenyl anion. Thus, we plan to extend the theoretical analysis to evaluate the mechanism and the energetics for the formation of these systems. In parallel, further experimental work will be made to determine the best chemical conditions for the cleavage of the C–C bond (e.g., by introducing a variety of substituents at the phenyl ring).

Experimental Section

All manipulations were carried out under nitrogen using conventional Schlenk techniques. Most starting materials were commercial products and were used without further purification unless otherwise noticed. Li_2PdCl_4 was dried at 80 °C under vacuum for 4 h before use. The following compounds were prepared according to the published procedures: 2-methylphenylmercuric chloride,[23] 4-methylphenylmercuric chloride,[23] and 2,4-dimethylphenylmercuric chloride.[24] 3-Methylphenylmercuric chloride and 3,5-dimethylphenylmercuric chloride were prepared using the same procedure reported for the cognate 2-methylphenylmercuric chloride.[23] NMR solvents were dried over activated 4-Å molecular sieves and degassed by several freeze–thaw cycles. Samples for NMR spectra were prepared under nitrogen. NMR spectra were recorded in CDCl$_3$ at 298 K using the solvent as internal standard (7.26 and 77.00 ppm, respectively, for ^{1}H and ^{13}C) on Bruker DRX500, DRX400, DPX300, DPX250, and AC300 spectrometers. Low-temperature NMR spectra were recorded in CD$_2$Cl$_2$. Assignments are based on 2D experiments (NOESY, COSY, ^{13}C–^{1}H correlation, ^{13}C–^{1}H long-range correlation). One or more asterisks indicate interchangeable assignments. Electrospray mass spectra were acquired using a PE-Sciex API 365 mass spectrometer (Sciex, Thornhill, ON, Canada) equipped with an ion spray interface for pneumatically assisted electrospray. The compounds dissolved in dichloromethane ($\sim$1 g/L) were infused into the ion source at a flow rate of 5 L/min by a Harvard infusion pump (South Natick., MA). The ionization was obtained in positive ion mode. Electrospray conditions were as follows: nitrogen curtain gas, 1.25 L/min.; nebulizing gas (air), 1.16 L/min; ionspray voltage, 5500 V; orifice voltage, 35 V; ring voltage, 200 V. Full-scan single quadrupole mass spectra (10 scans) were acquired in the 70–700 u mass range; scan rate, 0.63 s; resolution W1/2 0.6. Electrospray ionization (ESI) of the arylbicycloheptylpalladium chloride dimers **5**–**9** in positive-ion mode led to the generation of [M – Cl]$^+$ ions. Owing to the isotopic abundance of chlorine (^{35}Cl 75.53%, ^{37}Cl 24.47%) and palladium (^{102}Pd 1.02%, ^{104}Pd 11.14%, ^{105}Pd 22.33%, ^{106}Pd 27.33%, ^{108}Pd 24.46%, ^{110}Pd 11.72%), the signal of the [M – Cl]$^+$ ion appeared like a cluster centered at *m/z* 618 for the monomethyl-substituted derivatives **5**, **7**, and **9** and at *m/z* 646 for the dimethyl-substituted complexes **6** and **8**.

Synthesis of Dimeric *cis,exo*-Arylbicycloheptylpalladium Chloride Complexes (5–9). General Procedure. Dry Li$_2$PdCl$_4$ (0.480 g, 1.83 mmol) was dissolved under nitrogen in freshly distilled CH$_3$CN (5 mL). The desired organomercuric salt (1.90 mmol) was added as a solid powder followed by a CH$_3$CN solution (3 mL) of 2-bicycloheptene (0.230 g, 2.45 mmol). When stirred at 0 °C for 3 h, the mixture turned from brown to yellowish. Stirring was continued for an additional 1 h at room temperature. The mixture was filtered under nitrogen on a medium sintered-glass funnel. The residue was washed twice with cooled CH$_3$CN (2 × 3 mL) and once with cooled diethyl ether (2 mL) and then dissolved by addition of small portions of CH$_2$Cl$_2$. The resulting solution was passed through Celite, and the solvent was removed under vacuum maintaining the flask at –10 °C. Recrystallization from CH$_2$Cl$_2$/pentane at –15 °C gave bright yellow flaky crystals which must be stored under nitrogen at low temperature (–15 °C).

cis,exo-3-(2′-Methylphenyl)-2-bicycloheptylpalladium Chloride Dimer (5). The title compound was obtained in 65% yield (0.390 g)

(22) Cámpora, J.; Gutiérrez-Puebla, E.; López, J. A.; Monge, A.; Palma, P.; del Río, D.; Carmona, E. *Angew. Chem.* **2001**, *113*, 3753.

(23) Nesmeyanov, A. N. *Chem. Ber.* **1929**, *62*, 1013.
(24) Benkeser, R. A.; Hickner, R. A. *J. Am. Chem. Soc.* **1958**, *80*, 5298.

according to the general procedure. ¹H NMR (300 MHz): δ 7.81 (br d, J = 7.6 Hz, 1H, H6′), 7.30−7.13 (m, 3H, H4′, H3′, H5′), 3.06 (br d, J = 10.0 Hz, 1H, H7 syn), 2.81 (d, J = 6.4 Hz, 1H, H3), 2.71 (s, 3H, CH₃), 2.32 (d, J = 3.3 Hz, 1H, H4), 2.24 (d, J = 3.9 Hz, 1H, H1), 1.58−1.42 (m, 3H, H5 exo, H2, H7 anti), 1.28−0.95 (m, 3H, H6 exo, H6 endo, H5 endo). ¹³C{¹H} NMR (75.4 MHz): δ 135.8 (C2′), 130.9 (C4′, C3′), 127.8 (C6′), 126.4 (C5′), 81.7 (C1′), 52.1 (C3), 41.3 (C1), 40.0 (C4), 38.8 (C7), 28.7 (C5), 27.9 (C2), 26.2 (C6), 21.3 (CH₃).

***cis,exo*-3-(2′,4′-Dimethylphenyl)-2-bicycloheptylpalladium Chloride Dimer (6).** The title compound was obtained in 66% yield (0.410 g) according to the general procedure. Recrystallization from CH₂Cl₂ at −15 °C gave crystals suitable for X-ray analysis. ¹H NMR (300 MHz): δ 7.73 (d, J = 8.0 Hz, 1H, H6′), 7.02 (br s, 1H, H3′), 6.97 (d, J = 8.0 Hz, 1H, H5′), 3.09 (d, J = 10.2 Hz, 1H, H7 syn), 2.76 (d, J = 6.3 Hz, 1H, H3), 2.67 (s, 3H, CH₃(C2′)), 2.31 (d, J = 3.1 Hz, 1H, H4), 2.26 (s, 3H, CH₃(C4′)), 2.22 (d, J = 3.6 Hz, 1H, H1), 1.60−1.43 (m, 3H, H5 exo, H2, H7 anti), 1.30−1.09 (m, 2H, H6 endo, H6 exo), 1.09−0.98 (m, 1H, H5 endo). ¹³C{¹H} NMR (75.4 MHz): δ 142.6 (C4′), 136.5 (C2′), 132.1 (C3′), 129.4 (C6′), 128.0 (C5′), 78.8 (C1′), 52.3 (C3), 41.9 (C1), 40.7 (C4), 39.6 (C7), 29.4 (C5), 28.0 (C2), 27.0 (C6), 22.0 (CH₃(C2′)), 21.8 (CH₃(C4′)).

***cis,exo*-3-(3′-Methylphenyl)-2-bicycloheptylpalladium Chloride Dimer (7).** The title compound was obtained in 75% yield (0.450 g) according to the general procedure. ¹H NMR (400 MHz): δ 7.49 (d, J = 7.0 Hz, 1H, H6′a), 7.46 (s, 1H, H2′b), 7.37−7.30 (m, 3H, H5′a, H6′b, H5′b), 7.24 (s, 1H, H2′a), 7.18 (br s, 1H, H4′b), 7.13 (d, J = 6.9 Hz, 1H, H4′a), 2.94 (d, J = 10.8 Hz, 1H, H7 syn), 2.83 (d, J = 6.1 Hz, 1H, H3), 2.58 (d, J = 3.1, 1H, H4), 2.46 (s, 3H, CH₃ b), 2.37 (s, 3H, CH₃ a), 2.34 (br s, 1H, H1), 1.62−1.52 (m, 1H, H5 exo), 1.48−1.35 (m, 2H, H2, H7 anti), 1.30−1.19 (m, 1H, H6 exo), 1.19−1.07 (m, 1H, H6 endo), 1.07−0.92 (m, 1H, H5 endo). ¹³C{¹H} NMR (100.6 MHz): δ 142.2 (C3′ a), 141.8 (C3′ b), 132.6 (C4′ b), 131.7 (C5′ a, C5′ b), 130.8 (C4′ a), 129.7 (C2′ b), 127.4 (C6′ a), 108.8 (C2′ a), 106.2 (C6′ b), 86.5 (C1′ b, C1′ a), 53.4 (C3), 42.3 (C1), 39.0 (C4), 38.2 (C7), 28.6 (C5), 27.2 (C6), 26.5 (C2), 22.4 (CH₃ a), 22.2 (CH₃ b).

***cis,exo*-3-(3′,5′-Dimethylphenyl)-2-bicycloheptylpalladium Chloride Dimer (8).** The title compound was obtained in 72% yield (0.450 g) according to the general procedure. ¹H NMR (400 MHz): δ 7.20 (s, 1H, H2′), 7.02 (s, 1H, H6′), 6.93 (s, 1H, H4′), 2.95 (d, J = 9.7 Hz, 1H, H7 syn), 2.82 (d, J = 7.2 Hz, 1H, H3), 2.60 (d, J = 3.1 Hz, 1H, H4), 2.40 (s, 3H, CH₃(C5′)), 2.34−2.27 (br s, 4H, CH₃(C3′), H1), 1.64−1.51 (m, 1H, H5 exo), 1.42 (d, J = 10.1 Hz, 1H, H7 anti), 1.38 (d, J = 6.2 Hz, 1H, H2), 1.29−1.08 (m, 2H, H6 exo, H6 endo), 1.04−0.94 (m, 1H, H5 endo). ¹³C{¹H} NMR (75.4 MHz): δ 142.7 (C5′), 142.4 (C3′), 132.5 (C4′), 126.3 (C6′), 104.7 (C2′), 87.7 (C1′), 53.2 (C3), 42.5 (C1), 38.9 (C4), 38.0 (C7), 28.6 (C5), 27.3 (C6), 26.0 (C2), 22.4 (CH₃(C3′)), 22.0 (CH₃(C5′)).

***cis,exo*-3-(4′-Methylphenyl)-2-bicycloheptylpalladium Chloride Dimer (9).** The title compound was obtained in 70% yield (0.420 g) according to the general procedure. ¹H NMR (300 MHz): δ 7.64 (d, J = 7.4 Hz, 1H, H2′), 7.42 (d, J = 5.2, 1H, H6′), 7.21 (br signal, 2H, H3′, H5′), 2.98 (d, J = 10.1 Hz, 1H, H7 syn), 2.78 (d, J = 7.2 Hz, 1H, H3), 2.53 (d, J = 3.5 Hz, 1H, H4), 2.30 (br s, 4H, CH₃, H1), 1.60−1.47 (m, 1H, H5 exo), 1.47−1.38 (m, 2H, H2, H7 anti), 1.29−1.06 (m, 2H, H6 exo, H6 endo), 1.06−0.92 (m, 1H, H5 endo). ¹³C{¹H} NMR (75.4 MHz): δ 142.1 (C4′), 132.7 (C3′*), 131.0 (C2′), 130.7 (C5′*), 110.8 (C6′), 82.0 (C1′), 53.3 (C3), 42.2 (C1), 39.1 (C4), 38.4 (C7), 28.6 (C5), 27.0 (C6), 26.7 (C2), 21.8 (CH₃).

The various methyl-substituted arylbicycloheptane derivatives were prepared by hydrogenolysis of the corresponding dimeric complexes **5**−**9**. Although these compounds have already been described,[25,26] ¹³C NMR data in CDCl₃ (which are lacking or given as mixture in the literature) are reported here.

***exo*-2-(2′-Methylphenyl)bicycloheptane.**[25,26] ¹³C{¹H} NMR (75 MHz): δ 145.5 (C1′), 136.2 (C2′), 130.2 (C3′), 125.6 (C5′), 125.2 (C4′), 124.7 (C6′), 43.8 (C2), 41.4 (C1), 38.7 (C3), 36.9 (C4), 36.3 (C7), 30.5 (C6), 29.1 (C5), 20.0 (CH₃).

***exo*-2-(3′-Methylphenyl)bicycloheptane.**[26] ¹³C{¹H} NMR (75.4 MHz): δ 147.5 (q), 137.6 (q), 128.1 (C5′), 127.9 (C2′), 126.1 (C4′), 124.0 (C6′), 47.2 (C2), 42.9 (C1), 39.1 (C3), 36.8 (C4), 36.1 (C7), 30.6 (C5), 28.9 (C6), 21.5 (CH₃).

***exo*-2-(4′-Methylphenyl)bicycloheptane.**[26] ¹³C{¹H} NMR (75.4 MHz): δ 143.6, 133.7, 127.8, 125.9, 45.9, 42.0, 38.1, 35.8, 35.0, 29.6, 27.9, 19.9.

***exo*-2-(2′,4′-Dimethylphenyl)bicycloheptane.**[26] ¹³C{¹H} NMR (75.4 MHz): δ 142.5 (q), 136.0 (q), 134.5 (q), 131.1 (C3′), 126.2 (C5′), 124.7 (C6′), 43.5 (C2), 41.6 (C1), 38.7 (C3), 36.9 (C4), 36.3 (C7), 30.5 (C6), 29.1 (C5), 19.7 (CH₃), 18.9 (CH₃).

***exo*-2-(3′,5′-Dimethylphenyl)bicycloheptane.**[26] ¹³C{¹H} NMR (75.4 MHz): δ 147.60 (q), 137.58 (2q), 124.93 (C2′, C6′), 47.18 (C2), 42.97 (C1), 39.04 (C3), 36.76 (C4), 36.12 (C7), 30.64 (C5), 28.91 (C6), 21.39 (2CH₃).

X-ray Crystallography. Crystal data and details of data collection are given in Table 2. A yellow block of **6**, mounted on a glass fiber with epoxy cement, was used for diffraction experiments carried out under a liquid nitrogen cold stream. Data were collected on a Siemens SMART CCD diffractometer equipped with rotating anode and controlled by the software SMART.[27] The radiation used was Cu Kα (λ = 1.5418 Å). For five setting of ϕ, narrow data "frames" were collected for 0.3° increments in ω. A total of 2500 frames of data were collected, affording a sphere of data. The crystals available were tiny and decayed quickly if exposed to air as well as to X-ray radiation. Data reduction was made with the program SAINT 4.0[28] by which an appropriate time decay correction was also applied. It is worth stressing the difficulties encountered to collect a suitable set of diffracted data. In fact, several attempts to collect data from the same crop of crystals were unsuccessful when a standard Enraf-Nonius CAD-4 diffractometer was used at room temperature.

The structure was solved by direct methods using the SIR97[29] package of programs. Refinement was made by full-matrix least squares on all F^2 data using SHELXL97.[30] At a later stage of refinement, hydrogen atoms were introduced at calculated positions. Anisotropic thermal parameters were used only for Pd and Cl atoms. An empirical absorption correction was applied by using the routines of the program XABS2.[31] One disordered molecule of the dichloromethane per dimeric complex was found in the crystal lattice. The two chlorine atoms are distributed at three tetrahedral apexes. Since two centrosymmetrically related molecules lie at a short contact distance (one Cl−Cl intermolecular distance is unreasonably short at ∼2.15 Å), it was concluded that is due to an intermolecular Cl⋯H hydrogen bonding. Accordingly, while one Cl and one H atom of CH₂Cl₂ were assigned a unitary population parameter, the parameter had to be halved for the other couple of H and Cl atoms. The treatment allows one to alternate the direction of the C−Cl⋯H−C bonding between the two solvent molecules with a reasonable Cl⋯H contact of 2.87 Å.

The poor quality of the data allowed us to refine only the Pd and Cl atoms with anisotropic thermal parameters while an overall temperature factor was assigned to the hydrogen atoms. The molecular drawing was made by using the program ORTEP-III for Windows,[32] and all

(25) Arcadi, A.; Marinelli, F.; Bernocchi, E.; Cacchi, S.; Ortar, G. *J. Organomet. Chem.* **1989**, *368*, 249.
(26) Olah, G. A.; Lee, C. S.; Prakash, G. K. S. *J. Org. Chem.* **1994**, *59*, 2590.
(27) SMART, Area-Detector Integration Software. Siemens Industrial Automation, Inc.: Madison, WI, 1995.
(28) SAINT, Version 4.0. Siemens Industrial Automation, Inc.: Madison, WI, 1995.
(29) SIR97. Altomare A., Burla M. C.; Camalli M.; Cascarano G. L.; Giacovazzo C.; Guagliardi A.; Moliterni A. G. G.; Polidori G.; Spagna R. *J. Appl. Crystallogr.* **1999**, *32*, 115.
(30) Sheldrick, G. M. *SHELXL97*, University of Gottingen, 1997.
(31) XABS2. Parkin, S.; Moezzi, B.; Hope H. *J. Appl. Crystallogr.* **1995**, *28*, 53.
(32) (a) ORTEP-III. Burnett, M. N.; Johnson, C. K., Report ORNL-6895; Oak Ridge National Laboratory, Oak Ridge, TN, 1996. (b) L. J. Farrugia, *J. Appl. Chem.,* **1997**, *30*, 565.

the computational work was performed by using the very user-friendly graphic interface of WINGX.[33]

Computational Details. All of the structures reported herein were optimized at the hybrid density functional theory (DFT) using the Becke's three-parameter hybrid exchange-correlation functional[34] containing the nonlocal gradient correction of Lee, Yang, and Parr[35] (B3LYP) within the Gaussian98 program.[12] All optimized structures were confirmed as minimums by calculation of numerical vibrational frequencies. A collection of Cartesian coordinates and total energies for all of the optimized molecules are available from the authors upon request. Basis set for the Pd atom utilized the effective core potentials of Hay and Wadt[36] with the associated double-ζ valence basis functions. The basis set used for the remaining atomic species was the 6-311G

one with the important addition of the polarization functions (d, p) for all atoms, including hydrogens.

Supporting Information Available: Additional crystal data for complex **6**. This material is available free of charge via the Internet at http://pubs.acs.org.

JA016587E

(33) L. J. Farrugia, *J. Appl. Chem.* **1999**, *32*, 837.
(34) Becke, A. D. *J. Chem. Phys.* **1993**, *98*, 5648.
(35) Lee, C.; Yang, W.; Parr, R. G. *Phys. Rev. B* **1988**, *37*, 785.
(36) Hay, P. J.; Wadt, W. R. *J. Chem. Phys.* **1985**, *82*, 299.